

Pacific Ocean Circulation Based on Observation

MASAKI KAWABE* and SHINZOU FUJIO

*Atmosphere and Ocean Research Institute, The University of Tokyo,
Kashiwanoha, Kashiwa, Chiba 277-8564, Japan*

(Received 31 August 2009; in revised form 15 February 2010; accepted 15 February 2010)

A thorough understanding of the Pacific Ocean circulation is a necessity to solve global climate and environmental problems. Here we present a new picture of the circulation by integrating observational results. Lower and Upper Circumpolar Deep Waters (LCDW, UCDW) and Antarctic Intermediate Water (AAIW) of 12, 7, and 5 Sv ($10^6 \text{ m}^3 \text{s}^{-1}$) in the lower and upper deep layers and the surface/intermediate layer, respectively, are transported to the North Pacific from the Antarctic Circumpolar Current (ACC). The flow of LCDW separates in the Central Pacific Basin into the western (4 Sv) and eastern (8 Sv) branches, and nearly half of the latter branch is further separated to flow eastward south of the Hawaiian Ridge into the Northeast Pacific Basin (NEPB). A large portion of LCDW on this southern route (4 Sv) upwells in the southern and mid-latitude eastern regions of the NEPB. The remaining eastern branch joins nearly half of the western branch; the confluence flows northward and enters the NEPB along the Aleutian Trench. Most of the LCDW on this northern route (5 Sv) upwells to the upper deep layer in the northern (in particular northeastern) region of the NEPB and is transformed into North Pacific Deep Water (NPDW). NPDW shifts southward in the upper deep layer and is modified by mixing with UCDW around the Hawaiian Islands. The modified NPDW of 13 Sv returns to the ACC. The remaining volume in the North Pacific (11 Sv) flows out to the Indian and Arctic Oceans in the surface/intermediate layer.

Keywords:

- Pacific Ocean,
- ocean circulation,
- meridional overturning,
- Lower and Upper Circumpolar Deep Waters,
- North Pacific Deep Water,
- Antarctic Intermediate Water,
- World Ocean Circulation Experiment.

1. Introduction

Ocean circulation plays prominent roles in the variation of global climate, the formation of layered characteristics in the ocean, and the sustenance of the marine environment by transporting water, heat, materials, larvae, etc. Clarifying the ocean circulation is therefore one of the most important tasks in oceanography. Mantyla (1975) and Mantyla and Reid (1983) presented Pacific and global distributions of deep-water properties near the sea bottom, suggesting rough views of near-bottom pathways of the deep circulation. Our understanding of global ocean circulation progressed to three-dimensional overall pictures, including flows in the surface and other layers, drawn by Gordon (1986), Broecker (1991), and Schmitz (1995). Those pictures, however, are too schematic for the Pacific Ocean, reflecting the fact that the Pacific Ocean circulation, in particular the deep circulation, is still not sufficiently well understood to allow researchers to acquire a precise and comprehensive view

of it. Detailed distributions of geostrophic current in the Pacific Ocean were reported by Reid (1997). Although informative and excellent, his figures have to be investigated further to obtain a more accurate picture of ocean circulation.

Our lack of understanding of deep circulation in the North Pacific is due to the difficulty of examination because of the vast expanse of the ocean basin, complex bottom topographies, and diluted water characteristics. However, in the last two decades, a number of observational studies of deep circulation in the Pacific Ocean have been carried out and regional understanding has greatly improved owing to the high-quality data of water properties and current velocity provided by the World Ocean Circulation Experiment (WOCE) and post-WOCE observations. In particular, it is important that such an observational study be performed for the region surrounded by Japan, Hawaii, and New Guinea, where the bottom topography is extremely complex (Fig. 1). It is therefore crucial to organize knowledge of the region and create a picture of the overall circulation in the Pacific Ocean, where meridional overturning circulation accompanied by upwelling occurs.

* Corresponding author. E-mail: kawabe@aori.u-tokyo.ac.jp

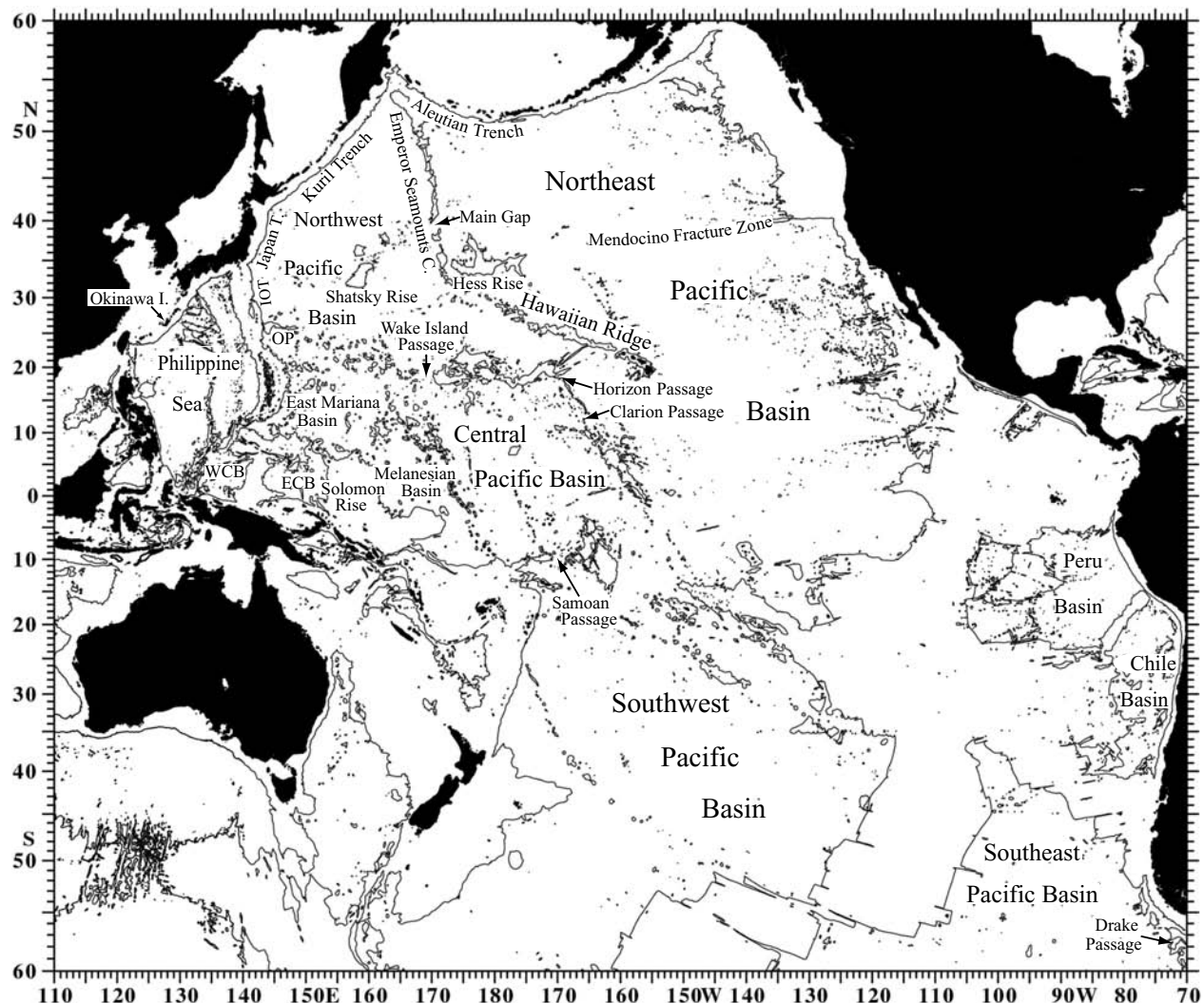


Fig. 1. Map of the Pacific Ocean. Thin lines show 4000-m isobaths. WCB: West Caroline Basin, ECB: East Caroline Basin, IOT: Izu-Ogasawara Trench, OP: Ogasawara Plateau.

In the present study the aim is to construct a more exact picture of the Pacific Ocean circulation than previous ones by integrating observational results obtained so far with information on upwelling volume transport estimated here. Overall circulation in the Pacific Ocean can be described comprehensively by the components of three layers: the lower and upper deep layers and the surface/intermediate layer. The layers north of the mid-latitude in the South Pacific almost correspond to potential temperature $\theta < 1.2^\circ\text{C}$ at depths greater than approximately 3500 m, $1.2\text{--}2.2^\circ\text{C}$ at depths of 2000–3500 m, and $\theta > 2.2^\circ\text{C}$ at depths less than 2000 m, respectively (e.g., Kawabe *et al.*, 2003), although the layers are demarcated by approximately 2.0°C and 3.0°C in the Antarctic Circumpolar Current.

2. Ocean Circulation in Lower Deep Layer Reaching the Northeast Pacific Basin

The Pacific Ocean circulation in the lower deep layer carries Lower Circumpolar Deep Water (LCDW), which is characterized by a salinity maximum and a silica minimum, being the remnant of North Atlantic Deep Water, although LCDW in the Pacific mostly comprises Antarctic Bottom Water (AABW), according to Johnson (2008). In the Antarctic Circumpolar Current, Circumpolar Bottom Water (CBW), which is characterized by lower salinity and lower chlorofluorocarbon than LCDW, exists at approximately $0.2\text{--}0.8^\circ\text{C}$ between LCDW above and AABW below (Orsi *et al.*, 1999). CBW and LCDW separating from the Antarctic Circumpolar Current flow northward along the western edge of the Southwest Pacific

Basin with a volume transport of 12–14 Sv ($10^6 \text{ m}^3 \text{s}^{-1}$), shown as 13 Sv in Fig. 2(c) (Warren and Voorhis, 1970; Wunsch *et al.*, 1983; Taft *et al.*, 1991; Tsimpis *et al.*, 1998). Whereas CBW is confined to the south of the Samoan Passage at 10°S (Orsi *et al.*, 1999), LCDW enters the Central Pacific Basin through the Samoan Passage and its vicinities with a volume transport of 6.0 Sv at the Samoan Passage (Rudnick, 1997) and 12 Sv in total (Roemmich *et al.*, 1996), proceeds further north, and finally reaches the Northeast Pacific Basin (Fig. 2(c)).

The pathway north of the Samoan Passage is complicated due to the complex bottom topography (Fig. 1). The deep circulation bifurcates into the western branch with 4 Sv and the eastern branch with 8 Sv (Johnson and Toole, 1993; Kawabe *et al.*, 2003, 2006). The western branch current is formed by an upper part of the deep circulation at depths of less than approximately 4500 m and carries LCDW warmer than 0.98°C , while the eastern branch is formed mainly by a lower part of the deep circulation below 4500 m, intensifying bottomward (Kawabe *et al.*, 2003, 2005).

Immediately north of 10°N , a branch current separates from the eastern branch current, proceeds eastward south of the Wake-Necker Ridge, and enters the Northeast Pacific Basin through the Horizon and Clarion Passages, mainly through the latter (Kato and Kawabe, 2009). The branch current carries LCDW colder than 1.05°C with a little less than 4 Sv. This is the southern (Hawaiian) route of LCDW to the Northeast Pacific Basin. A small amount of the LCDW detours cyclonically around the Hawaiian Ridge and moves northward along the western boundary of the Northeast Pacific Basin, as suggested by the low silica distribution (Talley, 2007) and the geostrophic velocity (Talley *et al.*, 1991).

The eastern branch current at the western edge of the Central Pacific Basin flows further north to enter the Northwest Pacific Basin through the Wake Island Passage and the western small channels with a little more than 4 Sv (Kawabe *et al.*, 2003, 2005). It then turns cyclonic in the basin between the Shatsky and Hess Rises (Kawabe and Taira, 1995; Yanagimoto and Kawabe, 2007) and flows westward south of the Shatsky Rise with slightly less than 4 Sv (Kawabe *et al.*, 2009), shown as 4 Sv in Fig. 2(c).

A small part of the eastern branch current separates at 30°N , 170°E , proceeds northward, enters the Northeast Pacific Basin through the Main Gap in the Emperor Seamounts Chain, and flows eastward over the northern slope of the Hess Rise (Hamann and Taft, 1987; Komaki and Kawabe, 2009). It joins the branch current coming from the southeast of the Hawaiian Ridge, and the confluence flows eastward south of the Mendocino Fracture Zone with volume transport of nearly 1 Sv (Kato and Kawabe, 2009).

The western branch current with approximately 4 Sv flows northwestward in the Melanesian Basin. It then flows northward in the East Mariana Basin, where half of it returns to the south and flows into closed basins, such as the Philippine Sea and the East Caroline Basin (Kawabe *et al.*, 2003; Siedler *et al.*, 2004). The remaining current with a little more than 2 Sv enters the Northwest Pacific Basin, passing east of the Ogasawara Plateau (Kawabe *et al.*, 2009), shown as 2 Sv in Fig. 2(c). The current flows northward along the Izu-Ogasawara and Japan Trenches and joins the eastern branch current around 38°N to the east of Japan (Fujio *et al.*, 2000; Fujio and Yanagimoto, 2005). These observations lead us to conclude that the confluence with approximately 6 Sv flows along the Kuril and Aleutian Trenches, as suggested by the large eastward flow along the Aleutian Trench shown by Warren and Owens (1988). It then reaches the northern region of the Northeast Pacific Basin, which is located north of the Mendocino Fracture Zone. This is the northern (Aleutian) route of LCDW to the Northeast Pacific Basin.

It should be noted that a cyclonic gyre is present in a trench that is composed of southward or westward (northward) current along the trench onshore slope and northward or eastward (southward) current along the offshore slope in the northern (southern) hemisphere. The trench gyre may be generated by the upwelling of the deep water supplied by the deep circulation (Johnson, 1998) or the blockage of the deep part of wind-forced gyre due to an ocean ridge or a continental slope (Kawabe, 2001). The deep circulation is distinct from the trench gyre, flowing on the offshore side (onshore flank) of trenches in the northern (southern) hemisphere, although Warren and Owens (1985, 1988), Owens and Warren (2001), and Hallock and Teague (1996) considered the southward or westward current on the onshore slope of the Aleutian, Kuril, and Japan Trenches to be the western boundary current of the deep circulation in the model of Stommel (1958).

LCDW on the northern route, in particular the converged LCDW in the northeastern region of the Northeast Pacific Basin, accumulates silica from bottom sediments in the Aleutian and Alaskan regions (Talley and Joyce, 1992; Johnson *et al.*, 2006), loses dissolved oxygen, and changes to “aged” water characterized by high silica and low dissolved oxygen. The LCDW containing more than $170 \mu\text{mol kg}^{-1}$ silica reaches the upper deep layer and occupies the entire deep layer north of 40°N , east of 150°W , forming the marked border of silica concentration at the Mendocino Fracture Zone ($\sim 40^\circ\text{N}$) with LCDW on the southern route, as shown in the sections of the WOCE Hydrographic Programme (WHP) P1, P16, and P17 (Talley, 2007). The LCDW on the southern route shows a similar vertical distribution with slightly less silica ($160\text{--}170 \mu\text{mol kg}^{-1}$) east of 140°W at 30°N (WHP

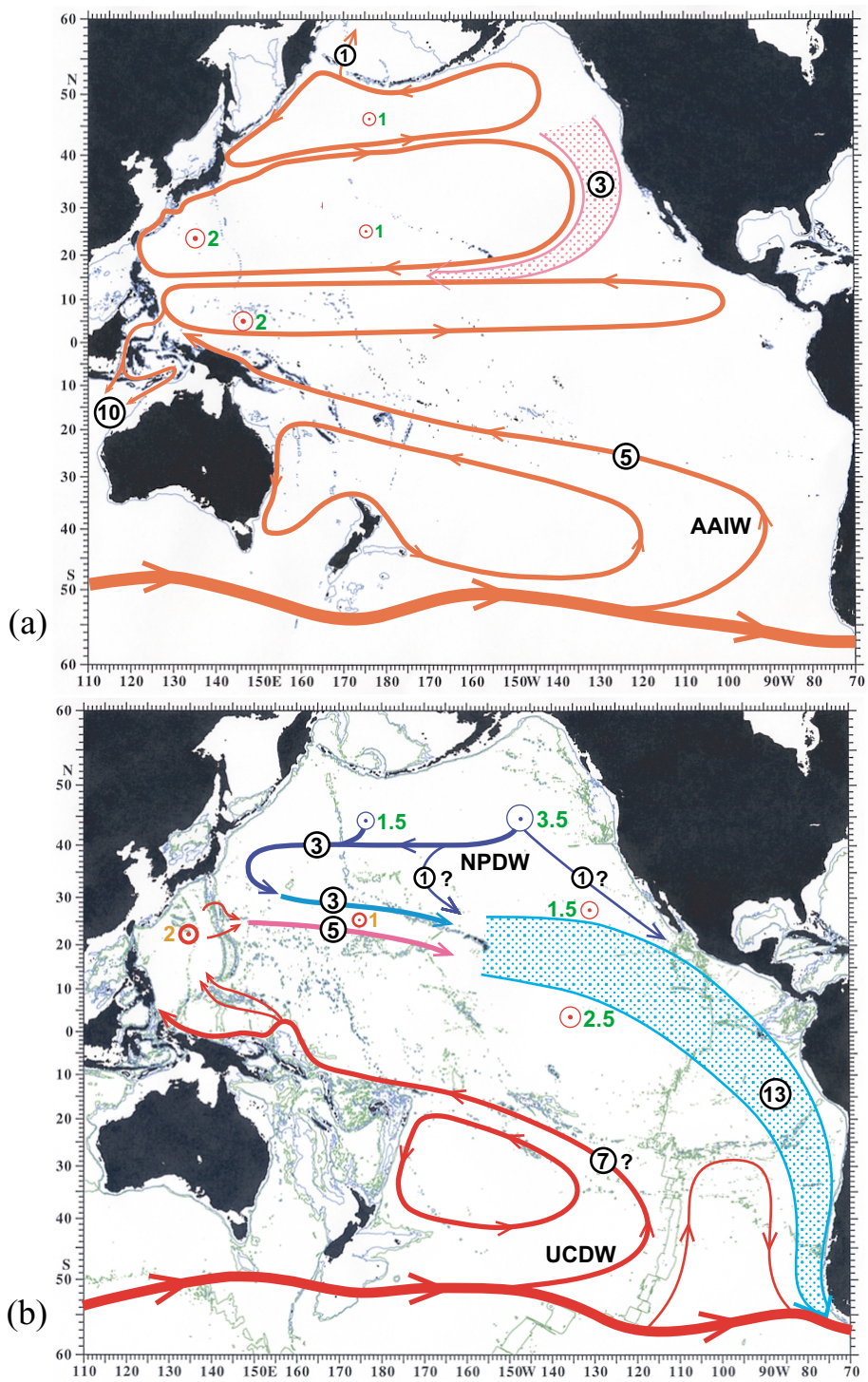


Fig. 2. Pacific Ocean circulation in the surface/intermediate layer (a), the upper deep layer (b), and the lower deep layer (c) carrying Antarctic Intermediate Water (AAIW), North Pacific Deep Water (NPDW), Upper Circumpolar Deep Water (UCDW), and Lower Circumpolar Deep Water (LCDW). The pink stippled arrow in (a) shows the flow due to subduction, forming a shallow salinity-minimum layer. The current in the Indonesian Islands with 10 Sv in (a) is the Indonesian Throughflow. The blue stippled arrow in (b) shows the flow carrying modified NPDW. Number in a circle shows volume transport of the current in $10^6 \text{ m}^3 \text{s}^{-1}$. The number 4^+ (4^-) means a little more (less) than 4 Sv. Bold (thin) circle with a center point shows upwelling from this layer to the upper layer (from the lower layer to this layer), its volume transport shown by a neighboring orange (green) number (Sv). Blue thin lines in (a) show 500-m isobaths, blue and green thin lines in (b) show 2000-m and 3000-m isobaths, and blue and green thin lines in (c) show 4000-m and 5000-m isobaths, respectively.

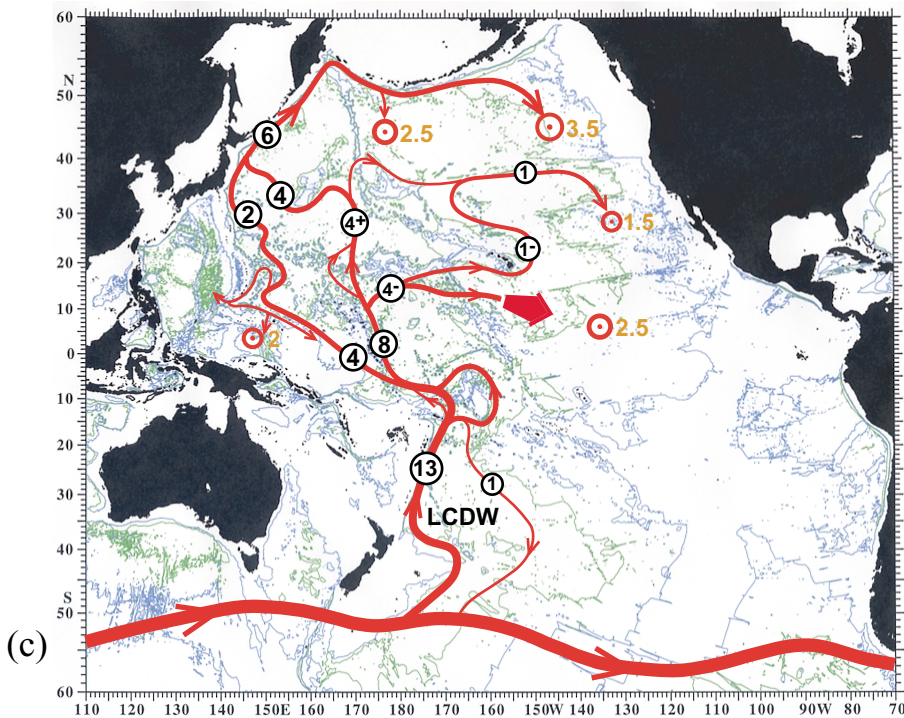


Fig. 2. (continued).

P2) and east of 130°W at 24°N (WHP P3) in the mid-latitude eastern region of the Northeast Pacific Basin. This suggests that LCDWs on the northern and southern routes do not join to form the border at the Mendocino Fracture Zone; rather, they upwell in the northeastern and mid-latitude eastern regions of the Northeast Pacific Basin, respectively. Thereafter, the upwelling LCDW is transformed into North Pacific Deep Water (NPDW) in the upper deep layer by further accumulating silica (Section 4).

3. Upwelling of LCDW

We now turn to an estimation of upwelling of LCDW. In the steady state in the sea, vertical advection and vertical diffusion are balanced in the conservation of potential density referred to the water pressure at each depth, taking the isopycnal surface (approximately the neutral surface) as the lateral surface; namely,

$$w \frac{\partial \sigma}{\partial z} = \frac{\partial}{\partial z} \left(K_V \frac{\partial \sigma}{\partial z} \right) \quad (1)$$

where z is the upward vertical coordinate; w , diapycnal velocity in the z direction; K_V , vertical (diapycnal) eddy diffusivity; and σ , potential density referred to an appropriate pressure in the deep layer. Equation (1) is written

as

$$\frac{\partial \xi}{\partial z} = \alpha \xi, \quad (2)$$

where $\xi = \partial \sigma / \partial z$ and $\alpha = (w - \partial K_V / \partial z) / K_V$. Equation (2) allows us to calculate α at each depth by calculating the vertical derivatives of σ . However, the second-order derivative of σ could not be precisely calculated and changes its sign vertically for actual data from conductivity-temperature-depth (CTD) profiler.

The solution of Eq. (2) on the boundary condition that $\xi = \xi_0$ at $z = z_0$ is

$$\ln \left(\frac{\xi}{\xi_0} \right) = \int_{z_0}^z \alpha(z) dz. \quad (3)$$

The term on the left-hand side is called the “stratification function” by Munk and Wunsch (1998), who showed that it increases upward with significant difference from a linear function of z . Then, α is assumed to be expressed by a quadratic function of z , namely,

$$\alpha = a(z - z_0)^2 + b(z - z_0) + c, \quad (4)$$

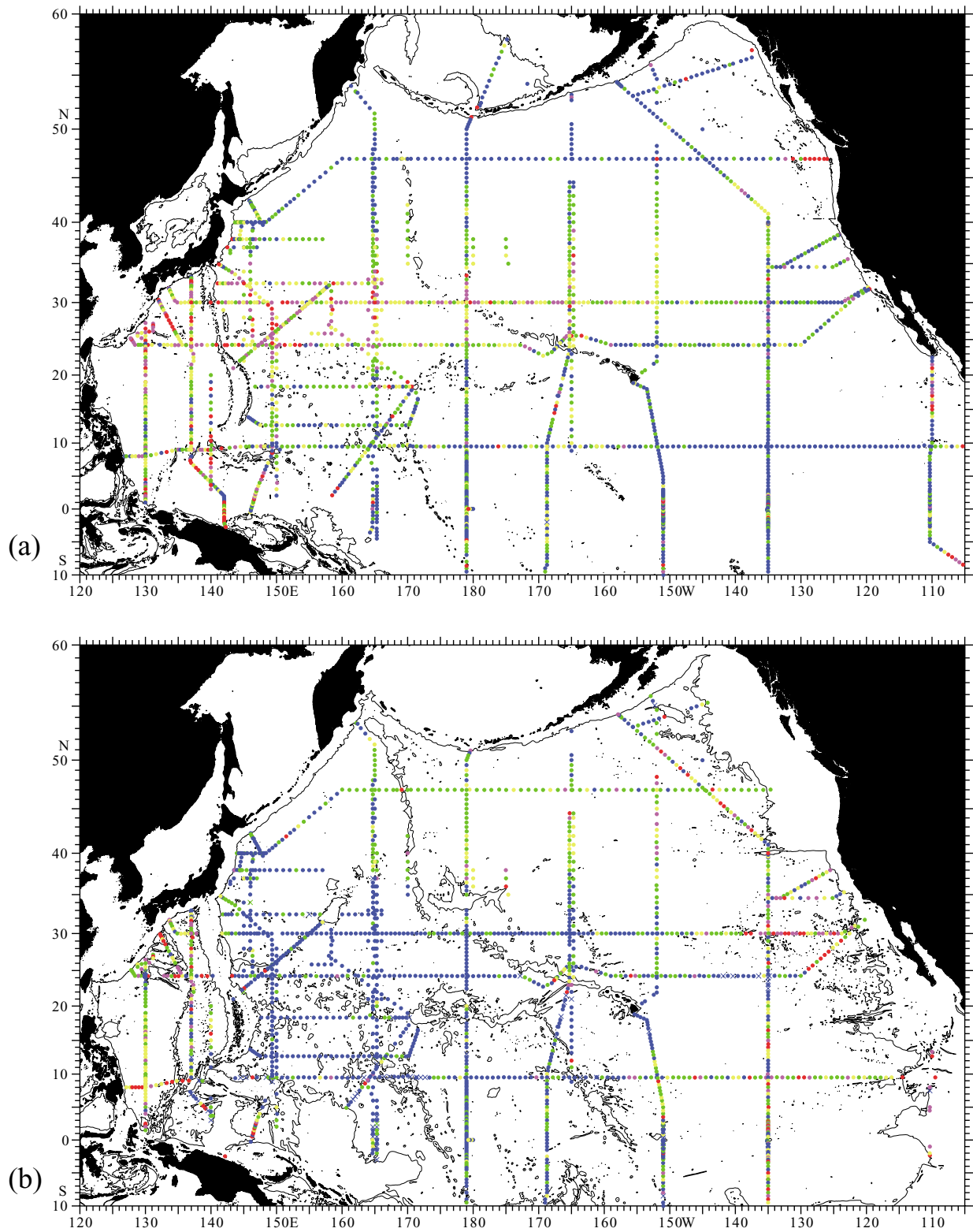


Fig. 3. Horizontal distribution of the vertical average of α ($= (w - \partial K_V / \partial z) / K_V$), $\bar{\alpha}$, in the layer of 1000–3000 m depth (a) and 3000–5000 m depth (b). α is calculated with potential density data from CTD at depths of 1000–3000 m (a) and greater than 3000 m except the 100-m bottom layer above the deepest data (b). Colors show the magnitude of $\bar{\alpha}$ (m^{-1}): (a) blue: $\bar{\alpha} < 10^{-3}$; green: $1.0-1.2 \times 10^{-3}$; yellow: $1.2-1.4 \times 10^{-3}$; magenta: $1.4-1.6 \times 10^{-3}$; red: $\bar{\alpha} \geq 1.6 \times 10^{-3}$. (b) Blue: $\bar{\alpha} < 10^{-3}$; green: $1.0-1.7 \times 10^{-3}$; yellow: $1.7-2.4 \times 10^{-3}$; magenta: $2.4-3.1 \times 10^{-3}$; red: $\bar{\alpha} \geq 3.1 \times 10^{-3}$. Thin lines show 2000-m (a) and 4000-m (b) isobaths.

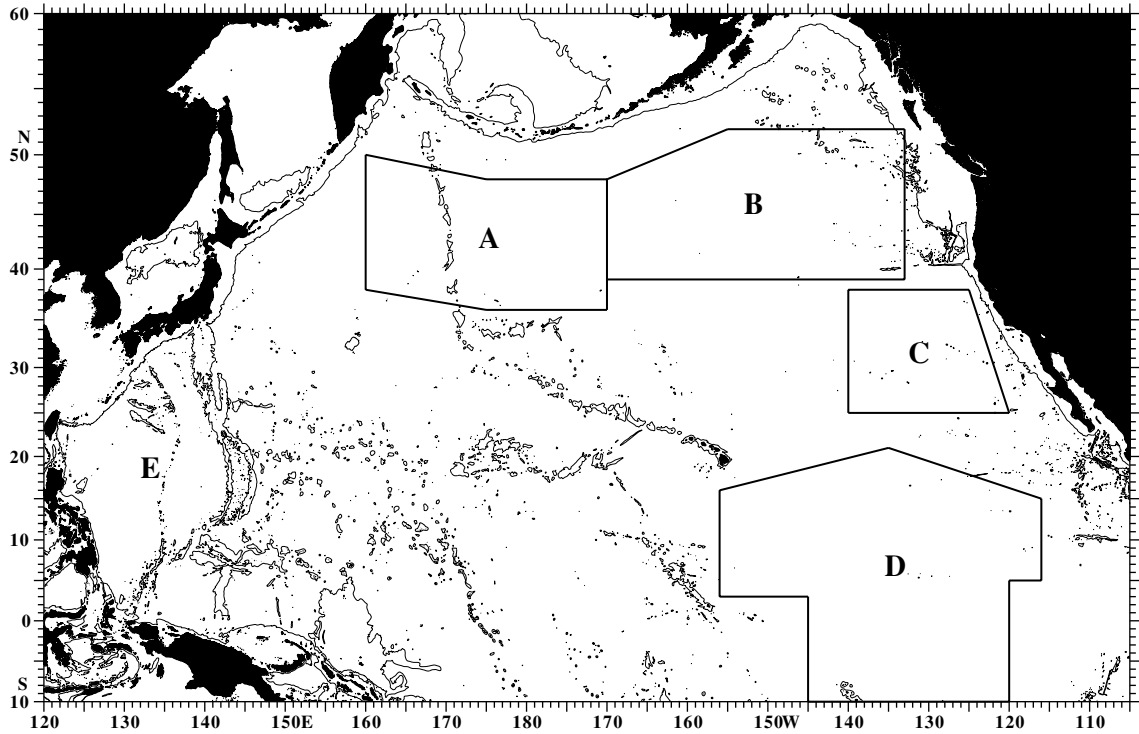


Fig. 4. Regions in which averaged $\bar{\alpha}$ and upwelling volume transport W , etc. are calculated. A. Northwestern Northeast Pacific Basin plus northeastern Northwest Pacific Basin (almost 36° – 48° N, 160° E– 170° W). B, C, D. Northeastern region (39° – 51° N, 170° – 133° W), mid-latitude eastern region (25° – 38° N, 140° – 122.5° W), southern region (5° – 18° N, 156° – 116° W and 17° S– 3° N, 145° – 120° W) of the Northeast Pacific Basin. E. Philippine Sea. Thin lines show 3000-m isobaths.

where a , b , and c are constants. By substituting Eq. (4) into Eq. (3), we obtain

$$\ln\left(\frac{\xi}{\xi_0}\right) = a'(z - z_0)^3 + b'(z - z_0)^2 + c'(z - z_0), \quad (5)$$

where $a' = a/3$, $b' = b/2$, and $c' = c$. The average of α between $z = z_1$ and $z = z_2$, $\bar{\alpha}$, is defined by

$$\begin{aligned} \bar{\alpha} &= \frac{1}{z_2 - z_1} \int_{z_1}^{z_2} \alpha dz \\ &= a'\left(\zeta_1^2 + \zeta_1 \zeta_2 + \zeta_2^2\right) + b'\left(\zeta_1 + \zeta_2\right) + c', \end{aligned} \quad (6)$$

where $\zeta_1 = z_1 - z_0$ and $\zeta_2 = z_2 - z_0$. $\bar{\alpha}$ is considered to be a typical value of α in the layer. Coefficients a' , b' , and c' are calculated from Eq. (5) by fitting to CTD data between $z = z_0$ and $z = z_2$ with the least-squares method, and $\bar{\alpha}$ is calculated from Eq. (6). In the present calculation, the depths z_2 , z_1 , and z_0 were taken to be 1000 m, 3000 m, and 3000 m for Fig. 3(a) and 3000 m, 5000 m, and the greatest depth of the data minus 100 m for Fig. 3(b), respectively.

The values of $\bar{\alpha}$ in the layer of 3000–5000 m are obtained for each CTD cast in the WHP and the Hakuho Maru cruises (KH-91-5, KH-93-2, KH-99-1, KH-03-1, KH-04-4, KH-05-4, KH-07-1, KH-08-3) (Fig. 3(b)). Although the depth z_0 in the calculation of $\bar{\alpha}$ is different in terms of water depth, the $\bar{\alpha}$ result does not depend on that. Overall, the values of $\bar{\alpha}$ are large in the Philippine Sea and the Northeast Pacific Basin but small in between. This implies that large $\bar{\alpha}$ is found in basins where UCDW and LCDW converge, whereas small $\bar{\alpha}$ is found in regions where the western boundary currents carrying LCDW flow. The value of $\bar{\alpha}$ is markedly large in the Northeast Pacific Basin, in particular its northeastern (B in Fig. 4), mid-latitude eastern (C), and southern (D) regions, and in the Philippine Sea (E), and is less (but not small) in the northeastern part of the Northwest Pacific Basin (western part of A). Large $\bar{\alpha}$ corresponds to almost uniform density at depths greater than 3500 or 4000 m in the Philippine Sea (Kawabe, 1993) and the Northeast Pacific Basin (Talley, 2007).

The remaining problem is the estimation of K_V and its vertical gradient, because upwelling velocity w is expressed by

$$w = \alpha K_V - w_d,$$

where w_d is $-\partial K_V/\partial z$ called the diffusive pseudo-velocity. w_d plays a similar role to vertical velocity in material conservations; upwelling w is depressed (intensified) by upwelling (downwelling) w_d . Although it is important to examine whether w_d is significant or not, the estimation of w_d is quite difficult. Moreover, w_d may be small in regions other than those around seamounts and ridges. w_d is thus ignored in the present study. This allows us to estimate upwelling velocity by multiplying α by K_V .

As there are few observations of K_V in the deep layer, K_V in wide regions is estimated with CTD data. Kunze *et al.* (2006) estimated K_V at several WHP sections based on a parameterization of internal waves by calculating shear and strain variances from lowered acoustic Doppler current profiler and CTD data, respectively. They concluded that K_V could be fairly calculated using only CTD data by assuming that the shear/strain variance ratio R_ω is 7. In this method, a factor with latitudinal dependence introduced by Gregg *et al.* (2003) is multiplied, but its validity has not been confirmed. Therefore, the calculation of K_V is attempted for the zonal sections at 47°N (WHP P1), 30°N (P2), 24°N (P3), and 10°N (P4). However, the calculation is not successful for WHP P1 and P3, because the CTD data obtained in the mid 1980s are too noisy to allow for the estimation of small-scale vertical variations. K_V at 47° and 24°N is estimated using WHP P1 and P3 revisit data obtained by the Japan Agency for Marine-Earth Science and Technology (Kawano and Uchida, 2007; Kawano *et al.*, 2009).

The values of R_ω and the factor of Gregg *et al.* (2003) could be different according to observed sites and the characteristics of the CTD sensors. The values of K_V can therefore not be obtained correctly by this calculation. K_V at 10°, 24°, and 30°N calculated with the method of Kunze *et al.* (2006) is therefore adjusted to match the resulting upwelling volume transport in the Philippine Sea with the expected value. Upwelling in the deep layer in the Philippine Sea occurs almost all in the upper deep layer, because there is little inflow in the lower deep layer (Johnson and Toole, 1993; Kawabe *et al.*, 2003). The lateral inflow to the Philippine Sea in the upper deep layer (2000–3500 m depth) is estimated to be 7 Sv, and one-third of it (2.33 Sv) is thought to enter at depths of 3000–3500 m and upwell at 3000 m depth (Section 4). This requires a K_V value of $2.88 \times 10^{-4} \text{ m}^2\text{s}^{-1}$ (Table 1). The values of K_V averaged at 3000–3500 m depths are multiplied by a factor to convert K_V in the Philippine Sea into this expected value. The K_V values averaged at every 5° longitude are shown in Fig. 5.

Zonal variations of K_V in Fig. 5 are apparently relevant because K_V is large around seamounts and ridges west of 170°E, 165°–160°W at 10°N; west of 150°E, around 165°W at 24°N; and west of 140°E, 150°–155°E, 175°E–170°W, east of 150°W at 30°N. Standard devia-

Table 1. Area and estimated values in regions A–E: α ($= (w - \partial K_V/\partial z)/K_V$) averaged at depths of 3000–5000 m ($\bar{\alpha}$), vertical eddy diffusivity K_V averaged at depths of 3000–3500 m, and upwelling volume transport W , assuming that $|w| \gg |\partial K_V/\partial z|$.

Region	Area ($\times 10^{12} \text{ m}^2$)	$\bar{\alpha}$ ($\times 10^{-3} \text{ m}^{-1}$)	K_V ($\times 10^{-4} \text{ m}^2\text{s}^{-1}$)	W (Sv)
A	3.32	1.66	3.5	1.93
B	4.02	2.17	3.5	3.05
C	2.42	2.69	1.28	0.833
D	12.5	2.16	0.734	1.98
E	3.61	2.24	2.88	2.33

tions of K_V in 5° longitude, indicating spatial variations of K_V , are also large in the seamount regions. On the other hand, K_V is uniformly small in ocean basins where the bottom topography is much less variable. The average values of K_V in the mid-latitude eastern region (C in Fig. 4) and the southern region (D) of the Northeast Pacific Basin are 1.3 and $0.73 \times 10^{-4} \text{ m}^2\text{s}^{-1}$, and the upwelling volume transport is 0.8 and 2.0 Sv, respectively (Table 1). This suggests that most of the LCDW on the southern route upwells in the region south of the Mendocino Fracture Zone in the Northeast Pacific Basin (Fig. 2(c)).

WHP P1 revisit at 47°N was performed in two cruises mainly west and east of 180°, and K_V cannot be estimated throughout the line. We thus adjusted K_V to make the values at common stations in these cruises similar. The result suggests that K_V is almost the same between A and B. However, the absolute values of K_V cannot be obtained using the present method for WHP P2, P3, and P4, because WHP P1 does not observe the Philippine Sea. We thus refer to the global averages of K_V calculated with inverse techniques by Ganachaud (2003) and Lumpkin and Speer (2007) ($3.7, 3.0 \times 10^{-4} \text{ m}^2\text{s}^{-1}$) and the averages in the Pacific deep and bottom layers ($4, 9 \times 10^{-4}$) reported by Ganachaud (2003). If K_V in A and B were $3.5 \times 10^{-4} \text{ m}^2\text{s}^{-1}$, the upwelling volume transport would be 1.9 Sv in A and 3.1 Sv in B (Table 1). Upwelling volume transport of LCDW on the northern route (6 Sv) is assigned as 2.5 Sv in A and 3.5 Sv in B (Fig. 2(c)).

4. Ocean Circulation in Upper Deep Layer

The upwelling of LCDW in the northeastern region of the Northeast Pacific Basin probably does not reach the surface/intermediate layer, as no water containing more than $170 \mu\text{mol kg}^{-1}$ silica is present above the upper deep layer in the sections of WHP P1, P16, and P17 (Talley, 2007) and $\bar{\alpha}$ in the 1000–3000 m layer is small (Fig. 3(a)). Upwelling aged LCDW further accumulates silica due to the dissolution of suspended particles in the

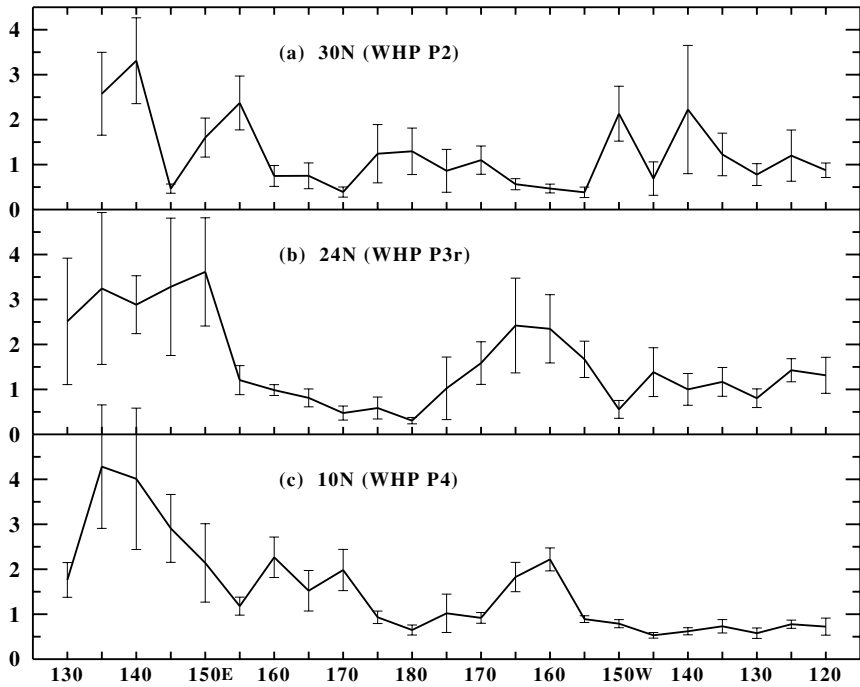


Fig. 5. Vertical eddy diffusivity K_V ($\times 10^{-4} \text{ m}^2 \text{s}^{-1}$) in the Pacific Ocean at 30°N, WHP P2 (a), 24°N, WHP P3 revisit (b), and 10°N, WHP P4 (c), averaged at depths of 3000–3500 m and at every 5° longitude. Calculated with potential density data from CTD using the method of Kunze *et al.* (2006) and adjusted to the expected values in the Philippine Sea as discussed in the text. Vertical thin lines show standard deviations of K_V in 5°-longitude regions.

upper deep layer (Talley and Joyce, 1992) and is transformed into North Pacific Deep Water (NPDW), characterized by high silica.

NPDW in region B spreads laterally in the upper deep layer (Fig. 2(b)). A large amount of NPDW proceeds westward, centered slightly north of 40°N, according to silica distribution (Johnson *et al.*, 2006) and lowered acoustic Doppler current profiler data (Komaki and Kawabe, 2007b); the remainder may proceed southward around 170°W and near the North American coast, as suggested by the high silica distribution on the WHP P2 line at 30°N (Talley, 2007). NPDW in B proceeding westward joins NPDW in A containing less silica than that in B, and the confluence turns cyclonic east of Japan. NPDW flows east-southeastward south of the Shatsky Rise at 30°–33°N with approximately 3 Sv (Kawabe *et al.*, 2009).

Another distinguishing property of the upper deep layer in the North Pacific is the inflow of Upper Circumpolar Deep Water (UCDW) from the Antarctic Circumpolar Current (Kawabe, 1993; Kawabe *et al.*, 2003). UCDW is transported by the anticyclonic flow in the South Pacific detouring around the subtropical gyre (Reid, 1997) and reaching the equatorial western Pacific. UCDW is defined as CDW with an oxygen minimum (Callahan, 1972) and the minimum oxygen structure is maintained from the Antarctic Circumpolar Current to

approximately 25°S (Reid, 1986; Tsuchiya and Talley, 1996; Wijffels *et al.*, 2001; Talley, 2007). However, on an isopycnal surface, dissolved oxygen in UCDW is higher than that in the surrounding water (Reid, 1986, 1997), and the pathway of UCDW can be inferred from a tongue of high dissolved oxygen in its lateral distribution. The concentration of dissolved oxygen, however, decreases greatly north of 15°S as UCDW proceeds northwestward from the Samoa Islands to New Guinea, and part of the lower-oxygen water returns southward by the western boundary current of the subtropical gyre (Reid, 1997).

UCDW enters the North Pacific passing east of the Solomon Rise (Kawabe *et al.*, 2006; Komaki and Kawabe, 2007a) and flows into the Philippine Sea by way of the East and West Caroline Basins and partly via the East Mariana Basin (Kawabe, 1993; Kawabe *et al.*, 2003). Volume transport of inflow to the Philippine Sea in the upper deep layer, carrying UCDW, was estimated to be approximately 10 Sv (Kawabe *et al.*, 2003, 2006), and 5 Sv out of it flows out from the northern part of the Philippine Sea (Kawabe *et al.*, 2009). This permits the conclusion to be drawn that the remaining UCDW of 5 Sv upwells to the surface/intermediate layer in the Philippine Sea. However, this amount of upwelling water may be too large.

Since 5 Sv of UCDW flows out from the Philippine Sea, the inflow volume transport of UCDW must be within 5–10 Sv. Part of it flowing into the Philippine Sea at depths of 3000–3500 m upwells to the layer shallower than 3000 m, because the Philippine Sea is almost completely closed at depths greater than 3000 m, except south of 12°N where UCDW flows in. Therefore, upwelling velocity increases upward in the layer of 3000–3500 m depth. Since this layer is the lower one-third of the upper deep layer, one-third of the total inflow of 5–10 Sv may flow into the Philippine Sea in this layer. Based on this assumption, the upwelling velocity increases and decreases upward in the layer of 2000–3000 m depth if the UCDW inflow is more and less than 7.5 Sv, respectively.

For more than 7.5 Sv, the deep current in the upper deep layer flows northward in the interior region of the Philippine Sea, where a vorticity balance between β and stretching terms is expected (Stommel, 1958); the resulting western boundary current is expected to flow southward. On the other hand, for the inflow less than 7.5 Sv, the deep current changes direction around a depth of 3000 m; the western boundary current flows southward and northward at depths greater and less than 3000 m, respectively. By performing measurements with moored current meters east of the Okinawa Island, Chaen *et al.* (1993) showed that the deep western boundary current in the Philippine Sea flows southwestward at depths greater than 3130 m, whereas it flows northeastward at depths less than 2650 m. This allows the conclusion that the UCDW inflow is less than 7.5 Sv.

If the UCDW inflow is 7 Sv, K_V at 2000–2500 m depth is estimated to be $3.03 \times 10^{-4} \text{ m}^2 \text{s}^{-1}$, using the factor for K_V obtained in Section 3. The value of $\bar{\alpha}$ at 1000–3000 m depths in the Philippine Sea is $1.38 \times 10^{-3} \text{ m}^{-1}$ on average (Fig. 3(a)). According to these values of K_V and $\bar{\alpha}$, the upwelling volume transport at 2000 m depth is 1.51 Sv, i.e., approximately 2 Sv. This is consistent with the UCDW inflow of 7 Sv and outflow of 5 Sv. Thus, the upwelling and inflow volume transports of UCDW are concluded to be 2 and 7 Sv, respectively (Fig. 2(b)).

East of the Izu-Ogasawara Trench, the characteristic waters, NPDW and UCDW, approach each other with a boundary at 27°–30°N and flow east-southeastward in parallel north and south of the boundary zone, respectively (Kawabe *et al.*, 2009). Contours of dissolved oxygen and silica on an isopycnal surface are markedly concentrated in the boundary zone, and the concentrated contours extend to the Hawaiian Ridge east-southeastward (Talley and Joyce, 1992; Kawabe, 1993). The concentration of the contours weakens greatly around the Hawaiian Islands, showing that NPDW and UCDW mix around that area and form modified NPDW. The value of $\bar{\alpha}$ is large in the region where NPDW and UCDW flow eastward (Fig. 3(a)). The average $\bar{\alpha}$ and K_V in the mid-lat-

tude North Pacific region (26° – 32° N, 142.5° E– 162.5° W; $3.52 \times 10^{12} \text{ m}^2$) are estimated to be $1.37 \times 10^{-3} \text{ m}^{-1}$ and $1.16 \times 10^{-4} \text{ m}^2 \text{s}^{-1}$, respectively, and the upwelling volume transport is estimated to be 0.56 Sv. Upwelling of nearly 1 Sv may occur in the region including the surrounding area (Fig. 2(b)).

A modified NPDW of 13 Sv is produced by NPDW (5 Sv), UCDW (5 Sv), and upwelling LCDW in regions C and D (4 Sv), minus the upwelling water in the mid-latitude North Pacific region (-1 Sv). Silica increases due to dissolution of sinking particles, but this effect may be neglected since the increase rate of $0.00073 \mu\text{mol L}^{-1} \text{yr}^{-1}$ east of Hawaii (Honjo *et al.*, 1982; Talley and Joyce, 1992) is quite small, sufficient to produce only an increase of $0.05 \mu\text{mol kg}^{-1}$ at most during the several decades it takes for the water to move from the subarctic to the subtropics. Water mixing leads us to expect that silica concentration in modified NPDW is $155 \mu\text{mol kg}^{-1}$ ($= (172.5 \mu\text{mol kg}^{-1} \times 5 \text{ Sv} + 140 \times 5 + 165 \times 1.5 + 145 \times 2.5 - 155 \times 1) \div 13 \text{ Sv}$), as silica concentration is 170–175 $\mu\text{mol kg}^{-1}$ for NPDW in A and B, 140 $\mu\text{mol kg}^{-1}$ for UCDW in the Philippine Sea, 165 and 145 $\mu\text{mol kg}^{-1}$ for LCDW in C and D, and 155 $\mu\text{mol kg}^{-1}$ around the boundary between NPDW and UCDW (Talley, 2007). This expected silica concentration ($155 \mu\text{mol kg}^{-1}$) is similar to that at 10° N in the eastern Pacific, which supports the hypothesis that modified NPDW is formed by the mixing of the waters.

Silica distributions in the sections of WHP P21 (17° S), P6 (32° S), and P17E (54° S) suggest that modified NPDW proceeds southward along the Middle and South American coast, significantly diluting the water characteristics, and flows back to the Antarctic Circumpolar Current in the vicinity of Drake Passage (Talley, 2007). The inflow of modified NPDW to circumpolar water creates or reinforces the oxygen minimum characteristic of UCDW (Callahan, 1972). This is supported by the fact that dissolved oxygen in circumpolar water is lowest at the WHP S1 line in the Drake Passage (Orsi and Whitworth, 2005).

The volume transport of modified NPDW (13 Sv) is similar to the southward volume transport of 10.9 Sv for depths of 2500–4200 m at 24° N, except the Philippine Sea, as estimated by Roemmich and McCallister (1989) (hereafter referred to as RM89). Shaffer *et al.* (2004) showed that the deep water with large negative radiocarbon, corresponding to modified NPDW, flowed southward east of 89° W at 32° S off the Chile coast with a geostrophic volume transport of approximately 10 Sv, using data of WHP P6E and direct current measurements. In addition, volume transport of the deep eastern boundary current at 32° S was estimated to be about 6 Sv by Tsimplis *et al.* (1998), 18 Sv by Wijffels *et al.* (2001), and 12 Sv by Sloyan and Rintoul (2001), using inverse models and

WHP data. The southward flow of modified NPDW with volume transport of 13 Sv in Fig. 2(b) does not seem too bad.

5. Ocean Circulation in Surface/Intermediate Layer

Water of 6 Sv upwells to the surface/intermediate layer in the subarctic gyre (1 Sv), the Philippine Sea (2 Sv), the mid-latitude North Pacific region (1 Sv), and the tropical closed basins (2 Sv) (Fig. 2(a)). The upwelling of UCDW in the Philippine Sea provides dissolved oxygen to shallower layers, at least to the intermediate oxygen-minimum layer, as dissolved oxygen at the oxygen minimum is much higher in the Philippine Sea than in the North Pacific. The upwelling in the tropical gyre occurs in closed basins, such as the West and East Caroline Basins, as suggested by Siedler *et al.* (2004) and Fig. 3.

Immediately north of the Antarctic Circumpolar Current, Subantarctic Mode Water is generated in the surface layer that is characterized by low salinity and high dissolved oxygen (McCartney, 1982). It is transported to the southeastern region of the South Pacific off Chile where it develops into a thick water mass with low salinity. This water mass is taken into the intermediate subtropical gyre where it produces a salinity minimum around a depth of $27.1\sigma_0$. The water around the salinity minimum is named Antarctic Intermediate Water (AAIW). This AAIW is carried by the intermediate anticyclonic current outside the subtropical gyre and the intermediate New Guinea Coastal Undercurrent (Reid, 1965, 1986, 1997), and then flows into the North Pacific, crossing the equator at 135°E (Tsuchiya, 1991; Zenk *et al.*, 2005).

Volume transport of AAIW carried by the intermediate New Guinea Coastal Undercurrent is estimated to be approximately 5 Sv (Tsuchiya, 1991). This value corresponds to the estimation of volume transport of the intermediate water across 32°S by inverse experiments constraining meridional silica fluxes (Sloyan and Rintoul, 2001). Part of the AAIW may leak to the east before crossing the equator, but may be compensated by South Pacific Tropical Water carried by the subsurface New Guinea Coastal Undercurrent (Tsuchiya *et al.*, 1989). Therefore, most AAIW of 5 Sv enters the North Pacific.

AAIW of 5 Sv and upwelling water of 6 Sv flow into the surface/intermediate layer in the North Pacific. The total water of 11 Sv flows out to the Arctic Ocean via the Bering Strait Throughflow, which has a volume transport of 0.83 Sv (Roach *et al.*, 1995), and to the Indian Ocean via the Indonesian Throughflow, which has 10–15 Sv (Gordon, 2001) and 9.5 Sv on average (Wijffels *et al.*, 2008). Volume transports of the Bering Strait and Indonesian Throughflows are shown as 1 and 10 Sv in Fig. 2(a), respectively.

Water volume upwelling in the subtropical gyre (3 Sv or less) has to be transported to the tropical gyre be-

fore flowing out to the Indian Ocean. This may occur through the southward current generated by subduction due to Ekman pumping in the region between the subtropical and subarctic ocean gyres in the northeastern part of the North Pacific. Surface water of approximately $26.0\sigma_0$ is subducted in the northeastern Pacific and flows southward along the North American coast, forming a shallow salinity-minimum layer (Reid, 1973). This water flows into the intermediate tropical gyre around $26.2\sigma_0$ and forms the shallow salinity-minimum layer at $25.8\text{--}26.5\sigma_0$, which has a thickness of approximately 150 m (Kawabe and Taira, 1998). RM89 estimated southward transport crossing 24°N at $26.0\text{--}26.8\sigma_0$ to be $1.7 \times 10^6 \text{ m}^2\text{s}^{-1}$ per 100 m in thickness (their figure 4a). Therefore, volume transport of the subducted flow is roughly estimated to be 2.6 Sv. This is similar to the upwelling volume transport in the subtropical gyre. The water subducted and transported to the tropics may be compensated by the water upwelling in the subtropical gyre.

6. Comparison with Past Work on Pacific Ocean Circulation

The map of deep currents at 5000 dbar in Reid (1997) shows the northward western boundary current in the Southwest Pacific Basin and the eastern and western branch currents bifurcating in the Central Pacific Basin, as in Fig. 2(c). However, the currents north of 10°N are different from those in Fig. 2(c), as pointed out by Yanagimoto and Kawabe (2007), Komaki and Kawabe (2009), and Kato and Kawabe (2009). First, Reid's map does not show the branch current south of the Hawaiian Ridge on the southern route of LCDW. Second, LCDW flowing on the northern route turns around east of the dateline, passes the Main Gap of the Emperor Seamounts Chain southwestward, and flows out from the Northeast Pacific Basin. Third, the current passing the Main Gap and the eastern branch current of the deep circulation turn east and flow eastward north of the Wake-Necker Ridge into the Northeast Pacific Basin.

Due to the second difference mentioned above, the upwelling of LCDW from the lower deep layer in regions A and B is not shown in the work of Reid (1997). Rather, downwelling occurs to supply water from the upper layer, as streamlines start from the Aleutian and Alaskan coasts in Reid's map. In regard to the third difference mentioned above, the eastward current in Reid's map is blocked around 30°N by the eastern slope in the Northeast Pacific Basin, producing an upwelling. These may lead to the unrealistically strong vertical cell in the meridional overturning streamfunction calculated on the basis of Reid's (1997) results by Talley *et al.* (2003). This vertical cell is composed of strong upwelling at $24^\circ\text{--}35^\circ\text{N}$ and strong downwelling north of 35°N . Based on the deep circulation in Fig. 2(c), meridional overturning must be

accompanied by significant upwelling north of 38°N and moderate upwelling around 30°N and at 17°S–18°N.

Reid's maps of the upper deep layer are markedly different from Fig. 2(b), as pointed out by Kawabe *et al.* (2009). His maps do not show the eastward current from the Philippine Sea carrying UCDW, probably due to the absence of steric height data, nor the southward current at 0°–20°N in the eastern Pacific carrying modified NPDW. Instead, zonally extending gyres are present at low latitudes. These probably decrease southward transport at 0°–24°N in the work of Talley *et al.* (2003), so that the meridional overturning transport in the deep layer at 24°N is much smaller in the work of Talley *et al.* (2003) (3 Sv at most) than in the present study (6 Sv).

The small overturning transport in the deep layer at 24°N has also been calculated with inverse models by Ganachaud (2003) (1 Sv) and Lumpkin and Speer (2007) (3 Sv at most). On the other hand, using inverse models, the overturning transport at 24°N is calculated to be 7.5 Sv by RM89, and southward transport of NPDW at 24°N is calculated to be 6 Sv by Macdonald (1998), values which are comparable to the present conclusions. Moreover, northward volume transport of LCDW at 24°N in the present result (7 Sv) is intermediate between the 9.6 Sv calculated by RM89 and the 5 Sv by Macdonald (1998). Thus, the result of the overturning transport at 24°N of RM89 is consistent with the present result. However, the results at 35°N and 47°N of RM89 do not coincide with the present ones, and RM89 concluded that upwelling of the meridional overturning occurs in the western boundary region in the North Pacific to the east of Japan. Macdonald (1998) does not present any significant southward transport of modified NPDW. These several results are different from the present picture.

The results obtained by inverse techniques depend on the model; they change depending on the constraints in the inverse models, an initial guess of solution (reference levels for geostrophic calculation, error estimates), and hydrographic data used in the calculation. The inverse techniques, however, are sufficiently robust, giving dynamical consistency to the ocean circulation calculated with hydrographic data. They are expected to be useful for incorporating consistency into the picture based on observations.

In a numerical study, Ishizaki (1994) simulated deep currents in the lower deep layer south of 20°N in terms of separation into the eastern and western branch currents and further branching from the former current, as well as the relative strength between them. However, the reproduced volume transport is small, being two-thirds of the present study. In particular, the deep currents north of 20°N, entering the Northeast Pacific Basin, are quite weak, being one-third of the present value, and as a result the meridional overturning transport at 24°N is 3 Sv

at most. The author pointed out that the small transport may be due to the small K_V ($0.3 \times 10^{-4} \text{ m}^2\text{s}^{-1}$) and exclusion of the Indonesian Throughflow. Furthermore, Ishizaki (1994) did not reproduce the northward UCDW flow in the upper deep layer, instead finding that the western boundary current returns southward. Roussenov *et al.* (2004) used an isopycnic numerical model to describe a similar deep flow pattern. However, the northern route of LCDW was not reproduced (countercurrents existed), whereas the current on the southern route was extremely strong.

7. Conclusions

The present study has constructed a picture of the Pacific Ocean circulation, comprising water circulations in three layers and the connection among the layers due to upwelling. Details of the circulation are described in Fig. 2.

LCDW of 12 Sv and UCDW of 7 Sv are transported from the Antarctic Circumpolar Current to the North Pacific by the deep circulation in the lower and upper deep layers, and AAIW of 5 Sv, by the intermediate current. In total, circumpolar waters of 24 Sv reach the North Pacific crossing the South Pacific. The water budget is balanced by the return flow of modified NPDW to the Antarctic Circumpolar Current in the upper deep layer (13 Sv) and the outflow from the North Pacific to the Indian Ocean via the Indonesian Throughflow (10 Sv) and to the Arctic Ocean via the Bering Strait Throughflow (1 Sv) in the surface/intermediate layer.

The inflow of LCDW of 12 Sv in the lower deep layer separates into the eastern (8 Sv) and western (4 Sv) branches in the Central Pacific Basin. Nearly half of the eastern branch separates and flows south of the Hawaiian Ridge into the Northeast Pacific Basin. This is the southern route of LCDW. The remaining part of the eastern branch of LCDW flows further north in the Central Pacific Basin, enters the Northwest Pacific Basin, and joins the western branch of LCDW in the western region of the Northwest Pacific Basin. The confluence of LCDW (6 Sv) flows northward along the Japan and Kuril Trenches, and most of it enters the Northeast Pacific Basin along the Aleutian Trench. This is the northern route of LCDW to the Northeast Pacific Basin. The LCDW on the northern route is aged by accumulating silica from bottom sediments, and is bounded at the Mendocino Fracture Zone by the LCDW on the southern route, generating a distinct border of silica concentration.

Marked upwelling of LCDW to the upper deep layer occurs in the northwestern (A in Fig. 4), northeastern (B), mid-latitude eastern (C), and southern (D) regions of the Northeast Pacific Basin as well as the Philippine Sea (E). Vertical eddy diffusivity K_V of $2.9 \times 10^{-4} \text{ m}^2\text{s}^{-1}$ is required for the Philippine Sea, and K_V in C and D is estimated to

be 1.3 and $0.73 \times 10^{-4} \text{ m}^2\text{s}^{-1}$, respectively. The values of $\bar{\alpha}$ defined by Eq. (6) are also estimated; $\bar{\alpha}$ is large in the Philippine Sea and the Northeast Pacific Basin, where the density stratification in bottom layer is weak since little near-bottom water of the deep circulation reaches these ocean basins. Upwelling volume transport is then estimated by multiplying K_V , $\bar{\alpha}$, and the area of the region, assuming that the diffusive pseudo-velocity w_d is neglected. The result proves that a large portion of the LCDW on the southern route upwells in C and D. LCDW on the northern route converges in A and B, and most of it (5 Sv) upwells to the upper deep layer and is transformed into NPDW, which is characterized by high silica. The upwelling in A and B requires K_V of $3.5 \times 10^{-4} \text{ m}^2\text{s}^{-1}$, which is comparable to the global average of K_V estimated with an inverse model by Ganachaud (2003) and Lumpkin and Speer (2007).

NPDW from A and B, UCDW from the northern Philippine Sea, and upwelling LCDW in C and D produce modified NPDW of 13 Sv by water mixing. The modified NPDW returns to the Antarctic Circumpolar Current in the upper deep layer, thereby completing meridional overturning circulation in the deep layer. Shallower meridional overturning occurs due to the significant upwelling of UCDW in the Philippine Sea to the surface/intermediate layer. The Philippine Sea is a key area for the Pacific Ocean circulation, in particular for UCDW circulation.

The Pacific Ocean circulation proposed in the present study is faithfully reproduced from observational results. Future observations may lead to revisions of some of the present conclusions of the currents and upwelling. If future estimates reveal that K_V values in the northern Northeast Pacific Basin (A, B) and the Philippine Sea (E) are significantly different from the values adopted here, we will have to investigate the consistency of the upwelling volume transport in the Northeast Pacific Basin with the volume transport of LCDW on the northern and southern routes. Nevertheless, the present picture inspires ideas for observation and dynamic studies of ocean circulation and is useful for the improvement of inverse and numerical models, thereby contributing to the further advancement of our understanding of the ocean.

Acknowledgements

The authors are grateful to their colleagues at Atmosphere and Ocean Research Institute, The University of Tokyo, for observations and discussion of deep ocean circulation. They also thank Drs. T. Kawano and M. Fukasawa for supplying CTD data on the WHP P1 and P3 revisit cruises.

References

- Broecker, W. S. (1991): The great ocean conveyor. *Oceanography*, **4**, 79–89.
- Callahan, J. E. (1972): The structure and circulation of deep water in the Antarctic. *Deep-Sea Res.*, **19**, 563–575.
- Chaen, M., M. Fukasawa, A. Maeda, M. Sakurai and M. Takematsu (1993): Abyssal boundary current along the northwestern perimeter of the Philippine Basin. p. 51–67. In *Deep Ocean Circulation, Physical and Chemical Aspects*, ed. by T. Teramoto, Elsevier Sci. Publishers, Amsterdam.
- Fujio, S. and D. Yanagimoto (2005): Deep current measurements at 38°N east of Japan. *J. Geophys. Res.*, **110**, C02010, doi:10.1029/2004JC002288.
- Fujio, S., D. Yanagimoto and K. Taira (2000): Deep current structure above the Izu-Ogasawara Trench. *J. Geophys. Res.*, **105**, 6377–6386.
- Ganachaud, A. (2003): Large-scale mass transports, water mass formation, and diffusivities estimated from World Ocean Circulation Experiment (WOCE) hydrographic data. *J. Geophys. Res.*, **108**(C7), 3213, doi:10.1029/2002JC001565.
- Gordon, A. L. (1986): Intercean exchange of thermocline water. *J. Geophys. Res.*, **91**, 5037–5046.
- Gordon, A. L. (2001): Intercean exchange. p. 303–314. In *Ocean Circulation and Climate, Observing and Modelling the Global Ocean*, ed. by G. Siedler et al., Academic Press, London.
- Gregg, M. C., T. B. Sanford and D. P. Winkel (2003): Reduced mixing from the breaking of internal waves in equatorial ocean waters. *Nature*, **422**, 513–515.
- Hallock, Z. R. and W. J. Teague (1996): Evidence for a North Pacific deep western boundary current. *J. Geophys. Res.*, **101**, 6617–6624.
- Hamann, I. and B. A. Taft (1987): The Kuroshio extension near the Emperor Seamounts. *J. Geophys. Res.*, **92**, 3827–3839.
- Honjo, S., S. J. Manganini and J. J. Cole (1982): Sedimentation of biogenic matter in the deep ocean. *Deep-Sea Res.*, **29**, 609–625.
- Ishizaki, H. (1994): A simulation of the abyssal circulation in the North Pacific Ocean. Part I: Flow field and comparison with observations. *J. Phys. Oceanogr.*, **24**, 1921–1939.
- Johnson, G. C. (1998): Deep water properties, velocities, and dynamics over ocean trenches. *J. Mar. Res.*, **56**, 329–347.
- Johnson, G. C. (2008): Quantifying Antarctic Bottom Water and North Atlantic Deep Water volumes. *J. Geophys. Res.*, **113**, C05027, doi:10.1029/2007JC004477.
- Johnson, G. C. and J. M. Toole (1993): Flow of deep and bottom waters in the Pacific at 10°N. *Deep-Sea Res. I*, **40**, 371–394.
- Johnson, H. P., S. L. Hautala, T. A. Bjorklund and M. R. Zarnetske (2006): Quantifying the North Pacific silica plume. *Geochem. Geophys. Geosyst.*, **7**, Q05011, doi:10.1029/2005GC001065.
- Kato, F. and M. Kawabe (2009): Volume transport and distribution of deep circulation at 165°W in the North Pacific. *Deep-Sea Res. I*, **56**, 2077–2087.
- Kawabe, M. (1993): Deep water properties and circulation in the western North Pacific. p. 17–37. In *Deep Ocean Circulation, Physical and Chemical Aspects*, ed. by T. Teramoto, Elsevier Sci. Publishers, Amsterdam.
- Kawabe, M. (2001): Interannual variations of sea level at the Nansei Islands and volume transport of the Kuroshio due to wind changes. *J. Oceanogr.*, **57**, 189–205.

- Kawabe, M. and K. Taira (1995): Flow distribution at 165°E in the Pacific Ocean. p. 629–649. In *Biogeochemical Processes and Ocean Flux in the Western Pacific*, ed. by H. Sakai and Y. Nozaki, Terra Sci. Publishing Company, Tokyo.
- Kawabe, M. and K. Taira (1998): Water masses and properties at 165°E in the western Pacific. *J. Geophys. Res.*, **103**, 12941–12958.
- Kawabe, M., S. Fujio and D. Yanagimoto (2003): Deep-water circulation at low latitudes in the western North Pacific. *Deep-Sea Res. I*, **50**, 631–656.
- Kawabe, M., D. Yanagimoto, S. Kitagawa and Y. Kuroda (2005): Variations of the deep western boundary current in Wake Island Passage. *Deep-Sea Res. I*, **52**, 1121–1137.
- Kawabe, M., D. Yanagimoto and S. Kitagawa (2006): Variations of deep western boundary currents in the Melanesian Basin in the western North Pacific. *Deep-Sea Res. I*, **53**, 942–959.
- Kawabe, M., S. Fujio, D. Yanagimoto and K. Tanaka (2009): Water masses and currents of deep circulation southwest of the Shatsky Rise in the western North Pacific. *Deep-Sea Res. I*, **56**, 1675–1687.
- Kawano, T. and H. Uchida (2007): *WHP P03 Revisit Data Book*. JAMSTEC, Yokosuka, 207 pp.
- Kawano, T., H. Uchida and T. Doi (2009): *WHP P01, P14 Revisit Data Book*. JAMSTEC, Yokosuka, 211 pp.
- Komaki, K. and M. Kawabe (2007a): Structure of the upper deep current in the Melanesian Basin, western North Pacific. *La mer*, **45**, 15–22.
- Komaki, K. and M. Kawabe (2007b): Correction method for full-depth current velocity with lowered acoustic Doppler current profiler (LADCP). *J. Oceanogr.*, **63**, 995–1007.
- Komaki, K. and M. Kawabe (2009): Deep-circulation current through the Main Gap of the Emperor Seamounts Chain in the North Pacific. *Deep-Sea Res. I*, **56**, 305–313.
- Kunze, E., E. Firing, J. M. Hummon, T. K. Chereskin and A. M. Thurnherr (2006): Global abyssal mixing inferred from lowered ADCP shear and CTD strain profiles. *J. Phys. Oceanogr.*, **36**, 1553–1576.
- Lumpkin, R. and K. Speer (2007): Global ocean meridional overturning. *J. Phys. Oceanogr.*, **37**, 2550–2562.
- Macdonald, A. M. (1998): The global ocean circulation: a hydrographic estimate and regional analysis. *Prog. Oceanogr.*, **41**, 281–382.
- Mantyla, A. W. (1975): On the potential temperature in the abyssal Pacific Ocean. *J. Mar. Res.*, **33**, 341–354.
- Mantyla, A. W. and J. L. Reid (1983): Abyssal characteristics of the World Ocean waters. *Deep-Sea Res.*, **30**, 805–833.
- McCartney, M. S. (1982): The subtropical circulation of Mode Waters. *J. Mar. Res.*, **40** (Suppl.), 427–464.
- Munk, W. and C. Wunsch (1998): Abyssal recipes II: energetics of tidal and wind mixing. *Deep-Sea Res. I*, **45**, 1977–2010.
- Orsi, A. H. and T. Whitworth, III (2005): *Hydrographic Atlas of the World Ocean Circulation Experiment (WOCE)*. Volume 1: Southern Ocean. International WOCE Project Office, Southampton.
- Orsi, A. H., G. C. Johnson and J. L. Bullister (1999): Circulation, mixing and production of Antarctic Bottom Water. *Prog. Oceanogr.*, **43**, 55–109.
- Owens, W. B. and B. A. Warren (2001): Deep circulation in the northwest corner of the Pacific Ocean. *Deep-Sea Res. I*, **48**, 959–993.
- Reid, J. L. (1965): Intermediate waters of the Pacific Ocean. *Johns Hopkins Oceanogr. Stud.*, No. 2, Johns Hopkins Press, Baltimore, 85 pp.
- Reid, J. L. (1973): The shallow salinity minimum of the Pacific Ocean. *Deep-Sea Res. Oceanogr. Abst.*, **20**, 51–68.
- Reid, J. L. (1986): On the total geostrophic circulation of the South Pacific Ocean: Flow patterns, tracers and transports. *Prog. Oceanogr.*, **16**, 1–61.
- Reid, J. L. (1997): On the total geostrophic circulation of the Pacific Ocean: Flow patterns, tracers, and transports. *Prog. Oceanogr.*, **39**, 263–352.
- Roach, A. T., K. Aagaard, C. H. Pease, S. A. Salo, T. Weingartner, V. Pavlov and M. Kulakov (1995): Direct measurements of transport and water properties through the Bering Strait. *J. Geophys. Res.*, **100**, 18443–18458.
- Roemmich, D. and T. McCallister (1989): Large scale circulation of the North Pacific Ocean. *Prog. Oceanogr.*, **22**, 171–204.
- Roemmich, D., S. Hautala and D. Rudnick (1996): Northward abyssal transport through the Samoan passage and adjacent regions. *J. Geophys. Res.*, **101**, 14039–14055.
- Roussenov, V., R. G. Williams, M. J. Follows and R. M. Key (2004): Role of bottom water transport and diapycnic mixing in determining the radiocarbon distribution in the Pacific. *J. Geophys. Res.*, **109**, C06015, doi:10.1029/2003JC002188.
- Rudnick, D. L. (1997): Direct velocity measurements in the Samoan Passage. *J. Geophys. Res.*, **102**, 3293–3302.
- Schmitz, W. J. (1995): On the interbasin-scale thermohaline circulation. *Rev. Geophys.*, **33**, 151–173.
- Shaffer, G., S. Hormazabal, O. Pizarro and M. Ramos (2004): Circulation and variability in the Chile Basin. *Deep-Sea Res. I*, **51**, 1367–1386.
- Siedler, G., J. Holfort, W. Zenk, T. J. Müller and T. Csernok (2004): Deep-water flow in the Mariana and Caroline Basins. *J. Phys. Oceanogr.*, **34**, 566–581.
- Sloyan, B. M. and S. R. Rintoul (2001): The southern ocean limb of the global deep overturning circulation. *J. Phys. Oceanogr.*, **31**, 143–173.
- Stommel, H. (1958): The abyssal circulation. *Deep-Sea Res.*, **5**, 80–82.
- Taft, B. A., S. P. Hayes, G. E. Friederich and L. A. Codispoti (1991): Flow of abyssal water into the Samoa Passage. *Deep-Sea Res.*, **38** (Suppl.), S103–S128.
- Talley, L. D. (2007): *Hydrographic Atlas of the World Ocean Circulation Experiment (WOCE)*. Volume 2: Pacific Ocean. International WOCE Project Office, Southampton.
- Talley, L. D. and T. M. Joyce (1992): The double silica maximum in the North Pacific. *J. Geophys. Res.*, **97**, 5465–5480.
- Talley, L. D., T. M. Joyce and R. A. deSzoeke (1991): Transpacific sections at 47°N and 152°W: distribution of properties. *Deep-Sea Res.*, **38** (Suppl.), S63–S82.
- Talley, L. D., J. L. Reid and P. E. Robbins (2003): Data-based meridional overturning streamfunctions for the global ocean. *J. Climate*, **16**, 3213–3226.
- Tsimplis, M. N., S. Bacon and H. L. Bryden (1998): The circulation of the subtropical South Pacific derived from

- hydrographic data. *J. Geophys. Res.*, **103**, 21443–21468.
- Tsuchiya, M. (1991): Flow path of the Antarctic Intermediate Water in the western equatorial South Pacific Ocean. *Deep-Sea Res.*, **38** (Suppl.), S273–S279.
- Tsuchiya, M. and L. D. Talley (1996): Water-property distributions along an eastern Pacific hydrographic section at 135W. *J. Mar. Res.*, **54**, 541–564.
- Tsuchiya, M., R. Lukas, R. A. Fine, E. Firing and E. Lindstrom (1989): Source waters of the Pacific Equatorial Undercurrent. *Prog. Oceanogr.*, **23**, 101–147.
- Warren, B. A. and W. B. Owens (1985): Some preliminary results concerning deep northern-boundary currents in the North Pacific. *Prog. Oceanogr.*, **14**, 537–551.
- Warren, B. A. and W. B. Owens (1988): Deep currents in the central subarctic Pacific Ocean. *J. Phys. Oceanogr.*, **18**, 529–551.
- Warren, B. A. and A. D. Voorhis (1970): Velocity measurements in the deep western boundary current of the South Pacific. *Nature*, **228**, 849–850.
- Wijffels, S. E., J. M. Toole and R. Davis (2001): Revisiting the South Pacific subtropical circulation: A synthesis of World Ocean Circulation Experiment observations along 32°S. *J. Geophys. Res.*, **106**, 19481–19513.
- Wijffels, S. E., G. Meyers and J. S. Godfrey (2008): A 20-yr average of the Indonesian Throughflow: Regional currents and the interbasin exchange. *J. Phys. Oceanogr.*, **38**, 1965–1978.
- Wunsch, C., D. Hu and B. Grant (1983): Mass, heat, salt and nutrient fluxes in the South Pacific Ocean. *J. Phys. Oceanogr.*, **13**, 725–753.
- Yanagimoto, D. and M. Kawabe (2007): Deep-circulation flow at mid-latitude in the western North Pacific. *Deep-Sea Res. I*, **54**, 2067–2081.
- Zenk, W., G. Siedler, A. Ishida, J. Holfort, Y. Kashino, Y. Kuroda, T. Miyama and T. J. Müller (2005): Pathways and variability of the Antarctic Intermediate Water in the western equatorial Pacific Ocean. *Prog. Oceanogr.*, **67**, 245–281.